Acta Biomaterialia 113 (2020) 478–487

Contents lists available at ScienceDirect

Acta Biomaterialia

journal homepage: www.elsevier.com/locate/actbio

Full length article

Caudicles in vandoid orchids: A carotenoid-based soft material with unique properties

Yiwen Zhang[a], Suchun Ji[a], Nannan Jian[b], Kai Zhang[b,*], Xinqiang He[c,*], Huiling Duan[a,d,**]

[a] State Key Laboratory of Turbulence and Complex Systems, Department of Mechanics and Engineering Science, BIC-ESAT, College of Engineering, Peking University, Beijing 100871, People's Republic of China
[b] School of Aerospace Engineering, Beijing Institute of Technology, Beijing 100081, People's Republic of China
[c] School of Life Sciences, Peking University, Beijing 100871, People's Republic of China
[d] CAPT, HEDPS and IFSA Collaborative Innovation Center of MoE, Peking University, Beijing 100871, People's Republic of China

ARTICLE INFO

Article history:
Received 16 March 2020
Revised 8 June 2020
Accepted 2 July 2020
Available online 8 July 2020

Keywords:
Caudicles
Elasticity
Pollination
Carotenoid
Hydrogel

ABSTRACT

130 years ago, Darwin observed that caudicles in vandoid orchids possess considerable elasticity and further hypothesized that their elasticity serves to improve pollination efficiency. However, there has been no study that seeks to either quantitatively backup Darwin's hypothesis or characterize this natural material for practical use. Here we show that vandoid caudicles are a novel kind of soft material with extremely high extensibility (1190%), low modulus (160 kPa) and density lower than that of water. Vandoid caudicles contain carotenoids that attach to basal polymers through noncovalent interactions. Inspired by the chemical structure of caudicles, we synthesize calcium-alginate/polyacrylamide hydrogels supplemented with carotenoids and demonstrate that their strength as well as stretchability are enhanced twofold. Our findings identify a new carotenoid-based material system with unique properties that approach the current boundaries of the Ashby chart, demonstrating potential application of carotenoids as biocompatible reinforcing agent for hydrogels.

Statement of Significance

We have investigated the microstructure, mechanical properties and chemical components of vandoid caudicles as an elastic plant tissue and demonstrated a bio-inspired design that can enhance the elasticity of hydrogels. Existing research on vandoid caudicles are very few and mainly focus on their phylogenetics and developmental process, and the potential application of caudicles in the field of material sciences remains unexplored. Our results showed that caudicles are more stretchable than most natural and synthetic elastomers and have a modulus similar to hydrogels. Carotenoids, an important chemical component of caudicles, can be used as supplements to hydrogels to improve their strength and stretchability.

1. Introduction

The caudicle is a special plant tissue in the pollination apparatus that is only found in certain orchid species. Caudicles in vandoid orchids are especially remarkable because they are not made of cells and possess considerable elasticity in their native form [1]. 130 years ago, Darwin observed that vandoid caudicles are highly extended before they break apart during insect pollination and further hypothesized that their elasticity serves to improve pollination efficiency [2]. However, this intriguing plant tissue has attracted little academic interest ever since. A few relevant researches have demonstrated that vandoid caudicles originate from the lysis of lipid-synthesizing inner tapetal cells and contain unsaturated lipids [3–4]. Nevertheless, there has been no study that systematically characterizes the physical structure, mechanical properties and chemical content of this natural material for scientific and practical purposes.

* Corresponding authors.
** Corresponding author at: State Key Laboratory of Turbulence and Complex Systems, Department of Mechanics and Engineering Science, BIC-ESAT, College of Engineering, Peking University, Beijing 100871, People's Republic of China.
E-mail addresses: zhangkai@bit.edu.cn (K. Zhang), hexq@pku.edu.cn (X. He), hlduan@pku.edu.cn (H. Duan).

https://doi.org/10.1016/j.actbio.2020.07.005
1742-7061/

Hydrogels are highly absorbent polymeric networks that are widely used in biomedical and clinical settings because of their unique properties. Recently, substantial research interests have focused on modifying the conventional matrix composition of hydrogels by adding supplements that enhance mechanical properties of hydrogels through noncovalent interactions. Common supplements include short alkyl chains [5-8] and dimer fatty acids [9] which form hydrophobic interactions, urea and amino acid derivatives [10–13] which form hydrogen bonds, various cations [14–17] and polyelectrolytes [18–19] which form ionic interactions, and graphene derivatives [20,–21] which form π-π stacking interactions. Naturally derived compounds could potentially be useful hydrogel supplements because their inherent biocompatibility enables *in vivo* administration of hydrogels.

In this study, we show that vandoid caudicles are more stretchable than most natural and synthetic elastomers and have modulus similar to hydrogels. Furthermore, carotenoids as an important chemical component of vandoid caudicles can be used as supplements to hydrogels that improve their strength and stretchability.

2. Materials and methods

2.1. Plant material

Flowers of *Phalaenopsis aphrodite* 'Bigchili' were used in this study. The plants were cultivated on moss medium with water pH 6.5–7.0 and EC value below 0.15 ms/cm. Temperature was kept at 24–26 °C during daytime and 18–20 °C during nighttime. Light intensity was kept at 15,000–20,000 Lx. Humidity was kept at 60–80%.

2.2. Stereomicroscopy

Stereomicroscope (Leica S8AP0) was used to characterize the general morphology, development process and elastic properties of caudicles and associate structures. All operations were done using tweezers and blades.

2.3. Environmental scanning electron microscopy (ESEM)

Environmental Scanning Electron Microscope (ESEM) avoids modifying the natural surface of materials and allows for direct imaging of wet samples, making it a more suitable technique to image caudicles than SEM. Caudicles were separated from surrounding tissues under stereomicroscope with minimal stretch. They were then embedded in epoxy structural adhesive blocks (A:B = 1:1) and set at room temperature for 24 h to allow epoxy to harden. The blocks were subsequently immersed in liquid nitrogen for 2.5 h. As soon as being lifted out of the liquid nitrogen, the blocks were bent perpendicular to the caudicle axis in order to ensure brittle fracture of the caudicles. Thus, the cross-sections of the caudicles embedded in epoxy were exposed. ESEM (FEI Quanta 200F) was used to observe the microstructures of the caudicle cross-sections in low-vacuum mode. In addition, the microstructures of the surface of caudicles were similarly observed using ESEM: after being separated from surrounding tissues, the caudicles were directly placed on the microscope stage without embedment or brittle fracture.

2.4. Synthesis of hydrogels

Crosslinkers including methylenebisacrylamide (MBAA, industrial grade, Shanghai Vita) and calcium sulfate ($CaSO_4$, 99%, Sigma-Aldrich) were all used as received. Ammonium persulphate (APS, ≥98%, Sigma-Aldrich), as photo-initiator, was used diretly without further purification. Other reagents were directly used as received, including tetramethylethylenediamine (TEMED, 99%, Sigma-Aldrich), as crosslinking accelerator, acrylamide (AAm, 99.0%, Sigma-Aldrich), sodium alginate (SA, viscosity: 200 ± 20 mPa s, Sigma-Aldrich) and astaxanthin (A790025, J&K).

To a solution of acrylamide (AAm, 1.20 g, 12% w/w) and sodium alginate (SA, 0.2 g, 2% w/w) in deionized water (10.00 ml), 700 μl methylenebisacrylamide (MBAA, 0.23% w/w), 200 μl calcium sulfate ($CaSO_4$, 0.1 M), 102 μl ammonium persulphate (APS, 0.1 M), 10 μl tetramethylethylenediamine (TEMED) and astaxanthin (0 mg (0.00% w/w), 3 mg (0.03% w/w), 5 mg (0.05% w/w), 10 mg (0.10% w/w), 50 mg (0.50% w/w)) were gradually added at room temperature. The mixture was stirred for 5 min at the same temperature. The solution was poured into a glass mold and then covered with a glass plate. The hydrogel was cured in one step with ultraviolet light for 1 h (with 8 W power and 254 nm wavelength, UV Crosslinkers XL-1500).

2.5. Tensile test

In tensile test of caudicles, caudicles were separated from surrounding tissues under stereomicroscope with minimal stretch. They were then glued on both ends to two pieces of stainless steel foil using CA40H instant adhesive (3 M). This process was carefully done under stereomicroscope using toothpicks to prevent the adhesive from infiltrating the central part of the caudicles. Stainless steel foils (20 mm × 5 mm × 0.01 mm) were used as gripping intermediates to reduce the influence of centering error of the microtester grippings on experiment results. The samples were set at room temperature for 12 h to ensure the hardening of the adhesive.

Before the tensile test, the gauge length and average diameter of the unglued central segment of each caudicle were measured by stereomicroscope images using ImageJ. The tensile test was conducted on the MicroTester 5848 (Instron) with the 5 N force sensor. The test was conducted at a speed of 0.1000 mm/s. Load (F) and elongation ($\triangle l$) were simultaneously recorded with a capture interval of 10 ms until complete rupture occurred. A total of 11 caudicles were tested. Examples of sample preparation and testing process can be found in Fig. S1 and Movie S2.

The stress-strain (σ-ε) curves were obtained from the load-elongation (F-$\triangle l$) curves using the following relationship: $\sigma = F / A$, $\varepsilon = \triangle l / l_0$, where A is the initial cross-sectional area, and l_0 is the initial gauge length of the sample, measured before the test. The following parameters of each caudicle were calculated from the stress-strain curve: tensile strength, defined as the maximum stress; breaking strain, defined as the strain corresponding to maximum stress; maximum load; tensile elastic modulus, defined as the slope of the first linear segment on the stress-strain curve; and the slope of the second linear segment on the stress-strain curve. Tensile elastic modulus was fitted in the strain range of 0–30% for all samples. Slope of the second linear segment was fitted in the strain range of 200–400% for all samples.

Tensile test of hydrogels was conducted in the same way as above except the following differences: hydrogel pads were cut into rectangular blocks of approximately 15 mm × 3 mm × 3 mm by blades under stereomicroscope with minimal stretch; small pieces (5 mm × 5 mm) of rubber gloves were first glued on one end of stainless steel foils to facilitate the gluing of hydrogel; hydrogel blocks were kept saturated with water during the entire cutting, gluing and storage processes (the CA40H instant adhesive performed well even with residue water on the hydrogel surface); the initial gauge length and cross-sectional area of the unglued central segment of each hydrogel block were measured after the sample had been loaded onto the microtester grippings; the

test was conducted at a rate of 1.0000 mm/s; 9 hydrogel blocks containing no astaxanthin and 9 hydrogel blocks containing 0.5% (w/w) astaxanthin were tested; tensile elastic modulus was fitted in the strain range of 0–40%, 0–30% or 0–20% for all samples; slope of the second linear segment was fitted in the strain range of 100–150% for all samples.

2.6. Density measurement

We calculated the density of caudicles by measuring their mass and volume separately. In mass measurement, a total of 40 caudicles were carefully separated from surrounding tissues and examined under stereomicroscope to ensure structural integrity. They were then divided into 8 groups with 5 caudicles per group. Among the 8 groups, 4 of them were randomly selected at a time, and the mass of the 20 caudicles were measured with a digital analytical balance with 1 μg readability (Sartorius ME36S). Random selection and mass measurement are repeated 10 times. In volume measurement, stereomicroscope images and ESEM images of 7 caudicles were analyzed. The shapes of the caudicles were approximated to cylinders, and the height and average diameter of each caudicle were measured using ImageJ.

2.7. Raman spectroscopy

In Raman spectroscopy of caudicles, the caudicles were separated from the pollinia and the stipe with tweezers. In extraction experiments, caudicles were immersed in chloroform at room temperature for 24 h. After that, the insoluble fraction was lifted out by clean tweezers and left at room temperature until chloroform had fully evaporated. Treatment by acetone and ethanol was performed similarly. Lycopene powder (Sigma) and caudicles without chloroform treatment were tested on inVia Reflex (Renishaw) with 532 nm laser. The soluble and insoluble fraction after chloroform treatment as well as the insoluble fraction after acetone and ethanol treatment were tested on Micro Raman imaging spectrometer DXRxi (Thermo Fisher) with 532 nm laser. Baseline of the spectra was subtracted in OMNIC and peaks were analyzed in Origin.

In Raman spectroscopy of hydrogels, hydrogel pads were cut into rectangular blocks of approximately 15 mm × 3 mm × 3 mm by blades under stereomicroscope and were tested on Micro Raman imaging spectrometer DXRxi (Thermo Fisher) with 532 nm laser. Hydrogel blocks were kept saturated with water during the entire cutting and storage processes. Baseline of the spectra was subtracted in OMNIC and peaks were analyzed in Origin.

2.8. Fourier-transform infrared (FTIR) spectroscopy

Samples were prepared as in Raman spectroscopy experiments except that untreated caudicles and the insoluble fraction after treatment with chloroform were subjected to vacuum freeze-drying for 4 h and then placed near silica gel before testing. Caudicles without chloroform treatment were tested on LUMOS (Bruker). The soluble and insoluble fraction after extraction were tested on Spectrum Spotlight 200 FT-IR microscopy (PE). Baseline of the spectra was subtracted in OMNIC and peaks were analyzed in Origin.

2.9. UV–vis absorption spectroscopy

Caudicles were treated with chloroform at room temperature for 24 h. The soluble fraction was tested on Synergy H1 Hybrid Multi-Mode Reader (BioTek). Scanning range was set as 400–600 nm with step size of 10 nm.

2.10. Mass spectrometry (MS)

Nine caudicles were treated together with 1 ml chloroform at room temperature for 24 h. Lycopene (≥90%, Ke Lei Biological Technology) and astaxanthin (≥98%, Acmec) powder was separately dissolved in chloroform to make solutions with μM-level concentration. The soluble fraction after treating caudicles with chloroform, astaxanthin solution and lycopene solution were tested on MALDI-TOF/TOF Mass Spectrometer 5800 (AB Sciex). MALDI ion source and positive ion mode ($[M + H]^+$) was used. Scanning range was set as m/z range of 0–4000.

2.11. Weight change measurement after chloroform treatment

A total of ~50 caudicles were divided into 5 groups with ~10 caudicles per group. The total weight of each group before chloroform treatment was measured with a digital analytical balance with 0.01 mg readability (Sartorius CPA225D). Chloroform treatment was done as in Raman spectroscopy experiments. The insoluble fraction of each group was measured together using the same balance.

2.12. Water content measurement of caudicles

In order to reach an equilibrium swelling level, caudicles were immersed in deionized water for 24 h at room temperature. Then, caudicles were dried by the BIOBASE BK-FD10S freeze dryer at −60 °C for 48 h. The water content of caudicles at harvest was estimated as follows: *Water content at harvest* (w/w) = $(w_0\text{-}w_2)/w_0$; the water content of caudicles at saturation was estimated as follows: *Water content* (w/w) = $(w_1\text{-}w_2)/w_1$, where w_0 is the weight of untreated caudicles at harvest, w_1 is the weight of caudicles after water swelling and w_2 is the weight of caudicles after freeze drying.

2.13. Statistical analysis

Data were statistically analyzed using Origin. Tensile stress-strain curve of each replicate is first binned into strain window of 1% before averaging. Mechanical parameters are displayed as scatter dot plots. Differences between two groups were evaluated using two-tailed unpaired *t*-test. Differences between multiple groups were evaluated using one-way ANOVA and Tukey's honestly significant difference (HSD) post hoc test. A *p*-value less than 0.05 was used to define statistical significance (* $p < 0.05$, ** $p < 0.01$, *** $p < 0.001$).

3. Results

3.1. Elasticity of vandoid caudicles is manifested in hand pollination

In a typical vandoid orchid *Phalaenopsis Aphrodite*, the caudicles and related structures reside in a white pocket at the top of the column in the center of the flower (Fig. 1a and b). The pollinia are compact masses formed by the aggregation of pollen grains that are transported together by insects during pollination. Two pollinia are connected to the stipe by two caudicles. The stipe is further attached to the viscidium, a sticky disk that adheres to the back of pollinating insects. The caudicles are almost hidden from view in the notches of the pollinia and are only exposed when the pollinia are removed (Fig. 1c and d).

To test whether the elasticity of vandoid caudicles is manifested during biological processes, we performed hand pollination on *Phalaenopsis Aphrodite* (Movie S1). Under natural conditions, when an insect visits a vandoid orchid flower, the sticky viscidium adheres to its back, thereby loading the insect with pollinia. When

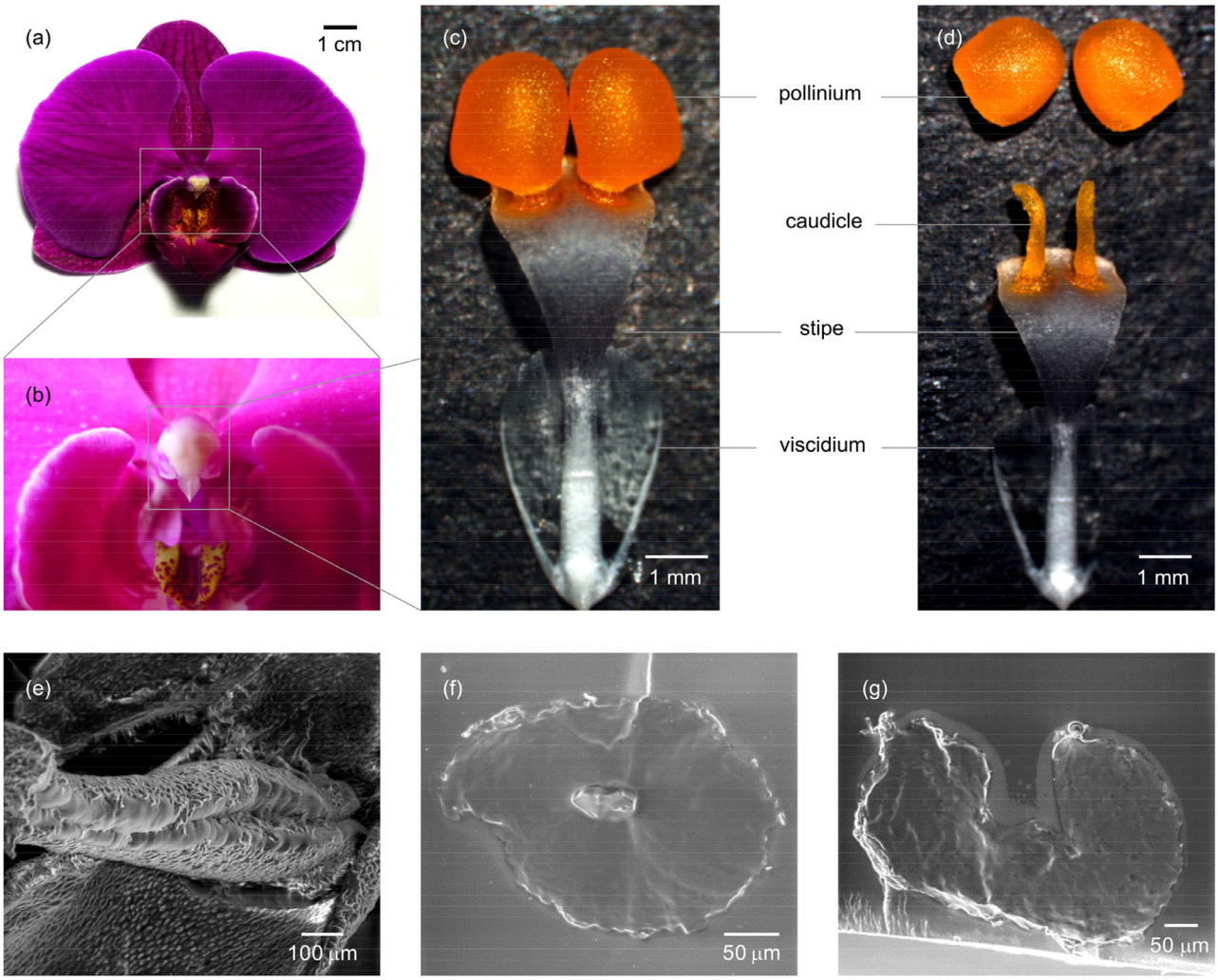

Fig. 1. Structure of vandoid caudicles and associate tissues. (a),(b) Pictures of the *Phalaenopsis aphrodite* flower. The gray box in (a) shows the portion of the flower that is highlighted in (b); the gray box in (b) shows where the caudicles and associate tissues reside, which is further inspected in (c) and (d). (c),(d) Stereomicroscope images of caudicles and associate structures. (e) Environmental scanning electron microscope (ESEM) image of a vertically placed caudicle standing on the stipe. (f),(g) ESEM images of cross-sections of caudicles exposed by brittle fracture.

the insect arrives at a second flower, the pollinia adhere to the stigma and eventually break away from the caudicles. To mimic the activity of insects, we adhered the viscidium to a stick and placed the pollinia within the stigma, simulating the insect docking on the flower. Then, similar to how the insect would fly away, we moved the stick upward. At this point, one of the two pollinia had been stuck in the stigma and could not move up with the stick. As a result, the caudicle that connected the pollinium to the stipe was stretched to multiple times its original length and became visible as an orange line. Finally, the caudicle was ruptured, leaving the pollinium in the stigma and thus completing pollination. Therefore, the elasticity of caudicles is indeed biologically relevant because it is manifested in the pollination process. As for the importance of such elasticity to pollination, Darwin proposed that the elasticity of vandoid caudicles functions to improve pollination efficiency by preventing pollinia loss during insect flight and by preventing pollinia from adhering to immature or impregnated stigmas [2].

3.2. Vandoid caudicles have homogenous inner structure

We then investigated the physical structure of vandoid caudicles and associate tissues. In ESEM image (Fig. 1e), the caudicle is shaped like a cylinder with ~1 mm in length and ~200 μm in diameter. Most of its surface is covered by protrusions 10–20 μm in size, but on one side there is a groove with smooth linings. To characterize the inner microstructure of vandoid caudicles, we observed the cross-sections of caudicles after brittle fracture. The cross-sections are surprisingly smooth with no discernable microstructure when imaged by ESEM, unlike the rugged surface of native caudicles (Fig. 1f and g). Therefore, vandoid caudicles have homogeneous inner structure on the micrometer scale, consistent with previous observations [4]. The protrusions on the surface of the caudicles are likely the result of molding effects that imprint onto caudicles the surface patterns of surrounding tissues and therefore do not reflect the intrinsic properties of the caudicles.

3.3. Morphology and elasticity of vandoid caudicles change during development

Vandoid caudicles have been shown to originate from the lysis of lipid-synthesizing inner tapetal cells during meiosis [3]. To characterize the structural changes of caudicles during later stages of flower development, we dissected floral buds of different sizes (Fig. 2). In the smallest stage-i buds, the caudicle is a gel-like, inelastic substance that is not clearly distinguishable from nearby

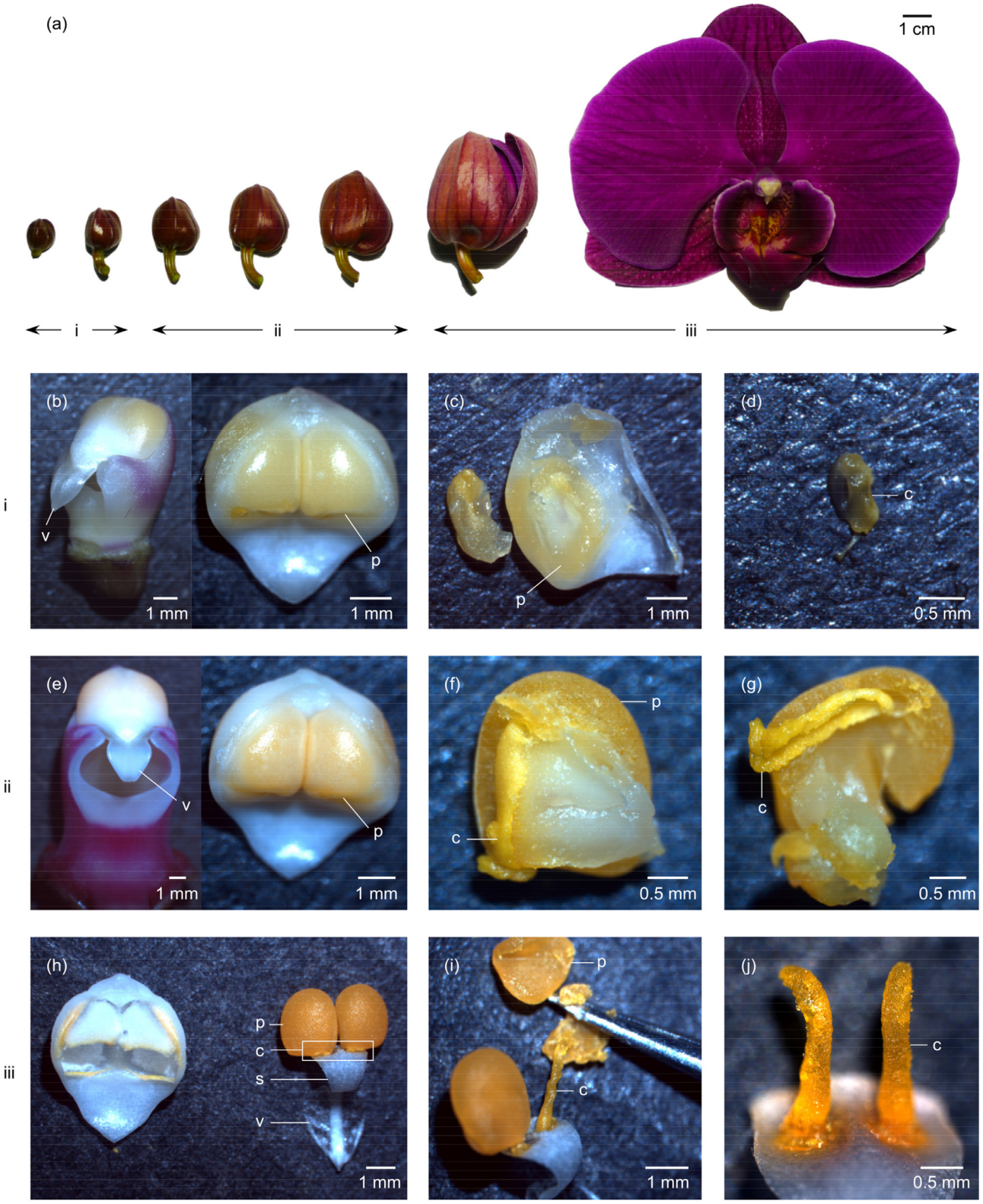

Fig. 2. Structure of vandoid caudicles and associate tissues during different developmental stages. (a) Picture of floral buds used in experiment. The buds were artificially grouped into three developmental stages (i, ii, iii) based on anatomic similarities. (b)–(d) Stereomicroscope images of the anatomy of buds in stage i. (e)–(g) Stereomicroscope images of the anatomy of buds in stage ii. (h)–(j) Stereomicroscope images of the anatomy of buds in stage iii. *v* = viscidium, *s* = stipe, *p* = pollinium, *c* = caudicle.

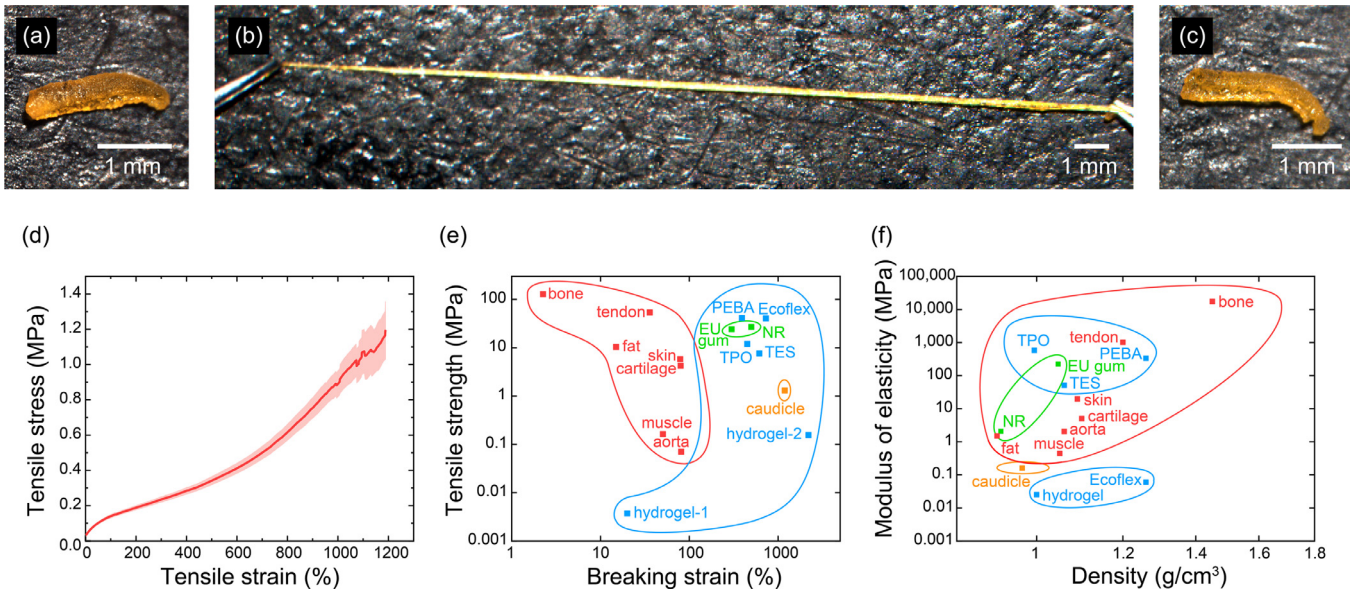

Fig. 3. Mechanical properties of vandoid caudicles and other materials. (a)–(c) Stereomicroscope images of a caudicle before (a), during (b), and after (c) being stretched with tweezers. (d) Average stress-strain curve measured by tensile test (mean ± SEM; $N = 11$). (e),(f) Comparison with other materials on breaking strain, tensile strength, density and modulus of elasticity. Green: plant-derived natural materials; red: animal tissues; blue: synthetic elastomers; orange: caudicle. Hydrogel-1 represents alginate hydrogel in [14]; hydrogel-2 represents calcium-alginate/polyacrylamide hydrogel in [14]. Border lines are drawn based on the location of data points and their error bars derived from the results of several studies. Density of hydrogels is seldom measured in literature and is therefore represented as density of water (1.0 g/cm^3). Material description and references can be found in Table S1. (For interpretation of the references to color in this figure legend, the reader is referred to the web version of this article.)

tissues (Fig. 2c and d); during stage ii, the caudicle has formed an entity with clear boundaries and has a groove that is entirely open on one side (Fig. 2g); during stage iii, the side groove on the caudicle is almost entirely closed, resulting in the mature cylinder-shaped caudicle (Figs. 2j and 1e). These changes suggest that the caudicle is initially synthesized as a sheet-like structure and gradually folds onto itself to form the cylinder-like structure. In addition, during stages i and ii, the pollinia are not yet connected to stipe and viscidium because the caudicles have not stretched out from the pollinia (Fig. 2b, c, e and f); during stage iii, the caudicles stretch out from the pollinia and tightly adhere to the stipe (Fig. 2h and i), therefore the perspective in stage iii is different from that in the first two stages.

3.4. Vandoid caudicles have uniquely high stretchability and low modulus

Next we demonstrated the extraordinary elasticity of vandoid caudicles as Darwin observed. We first stretched the caudicles using tweezers. The caudicle is able to be elongated to over ten times its original length without breaking, and can rapidly revert to its original length once the force is removed (Fig. 3a–c), thus showing their elasticity. We then performed tensile tests along the long axis of the caudicles to quantitatively characterize their elastic properties. Considering that the caudicles are very short in length (~1 mm), we used stainless steel foil as a gripping intermediate to reduce the influence of the centering error of the microtester grippings (see Materials and Methods, Fig. S1 and Movie S2). Several mechanical parameters can be derived from the stress-strain curve (Fig. 3d): the caudicle has tensile strength of 1.3 ± 0.2 MPa, maximum load of 114 ± 5 mN, breaking strain of 1190 ± 50% and tensile elastic modulus, defined as the slope of the first linear segment on the stress-strain curve, of 160 ± 20 kPa; the slope of the second linear segment on the stress-strain curve is 47 ± 4 kPa (mean ± SEM, $N = 11$). The density of caudicles is 0.97 ± 0.06 g/cm^3 (mean ± SEM, see Materials and Methods), lower than that of water.

We compared the mechanical parameters of vandoid caudicles with those of other natural and synthetic materials (Fig. 3e and f). Animal tissues generally have low breaking strain because tight junctions between cells prohibit large deformation. The caudicles, however, are not made of cells [1], and therefore possess large breaking strain. Hydrogel and Ecoflex, two synthetic elastomers known to be extraordinarily soft and "stretchy", are similar to caudicles in modulus; however, caudicles have lower density, and their breaking strain is larger than that of Ecoflex and alginate hydrogel (hydrogel-1) but smaller than that of calcium-alginate/polyacrylamide hydrogel (hydrogel-2) [14]. A detailed comparison between caudicles and other types of hydrogels can be found in Fig. S2 [22–24], also see supplementary references]. Natural rubber and *Eucommia ulmoides* gum (EU gum) are plant-derived natural materials processed from tree latex. Compared with them, the caudicles have lower elastic modulus, larger breaking strain and lower tensile strength. In conclusion, comparison with other materials more clearly portrays the vandoid caudicle as a soft natural material with high extensibility, low density and low modulus.

3.5. Vandoid caudicles contain noncovalently bound carotenoids

We then characterized the chemical structure of caudicles using spectroscopy methods. Raman spectrum of caudicles shows four strong bands that closely match the four bands of lycopene, a member of the carotenoid family (Fig. 4a, top two panels). Since most Raman bands of carotenoids are attributable to vibrations of the conjugated chain, Raman spectra of different carotenoid species are very similar [25]. Therefore, the above Raman spectrum indicates the abundant presence of carotenoids in caudicles. Carotenoids are a type of lipoidal small molecule with a polyene chain consisting of 9–11 conjugating double bonds and possible terminal rings. This result agrees with previous findings that unsaturated lipids are present in the caudicles [3–4].

We then tried to separate different fractions in caudicles by treating them with chloroform, a low-polarity solvent commonly used to extract lipids. Chloroform treatment yielded two fractions. One is the soluble fraction that changed from transparent to a yellow color, the other is the insoluble fraction that changed from

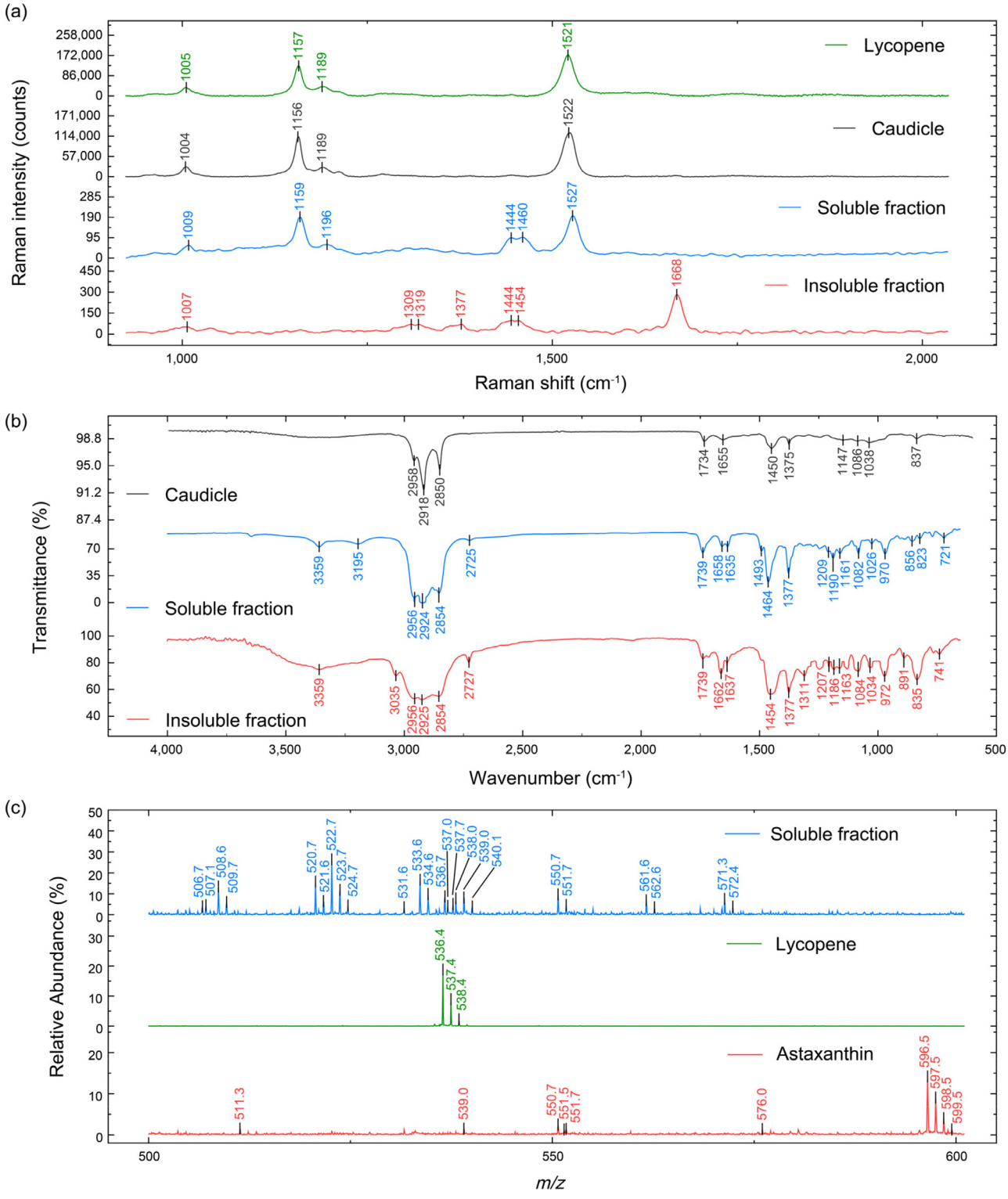

Fig. 4. Chemical composition of vandoid caudicles. (a) Raman spectra of lycopene (green), caudicle (black), soluble fraction (blue) and insoluble fraction (red) after treatment with chloroform. (b) Fourier-transform infrared (FTIR) spectra of caudicle (black), soluble fraction (blue) and insoluble fraction (red) after treatment with chloroform. (c) Mass spectrometry of the soluble fraction after treatment with chloroform. For (a)–(c), numbers indicate the position of peaks. (For interpretation of the references to color in this figure legend, the reader is referred to the web version of this article.)

orange to transparent. Compared with untreated caudicles, the insoluble fraction after treatment decreased 28 ± 4% (mean ± SEM, $N = 5$) in weight. The major Raman bands of carotenoids are present in the soluble fraction but not in the insoluble fraction (Fig. 4a, bottom two panels), indicating that chloroform treatment is able to extract out carotenoids from caudicles. This also suggests that carotenoids attach to basal polymer chains through weak intermolecular interactions but not covalent crosslinks. Notably, several Raman bands in 1300–1500 cm^{-1} and near 1668 cm^{-1} become visible in the insoluble fraction, indicating the presence of

saturated carbons and unconjugated carbon-carbon double bonds in basal polymers. Extracting with acetone and ethanol yielded similar results (Fig. S3). FTIR spectra do not change much after extraction, suggesting that methyl, alkenyl, carbonyl and hydroxyl groups are present in both soluble and insoluble fraction (Fig. 4b). UV–vis absorption spectrum also confirms the presence of carotenoids in the soluble fraction (Fig. S4).

Mass spectrometry is also performed to further characterize the soluble fraction (Fig. 4c). Apart from bands in the low *m/z* range which possibly result from the MALDI ion source, the major bands of the soluble fraction appear in the *m/z* range of 500–600, which is in the same range with major bands of lycopene and astaxanthin solutions. There is almost no signal in the high *m/z* range. This together with the above spectroscopy results indicates that carotenoids are the major component of the soluble fraction, and that carotenoid molecules exist as small molecule monomers in caudicles. Notably, there are multiple band groups near the *m/z* range of ~520, ~530, ~550, ~560 and ~570, indicating that there exist multiple species of carotenoid molecules. In summary, the caudicles contain a mixture of carotenoid monomers that bind to basal polymers through noncovalent interactions. The identity and relative abundance of individual carotenoid species in the caudicles remain unknown at the moment.

3.6. Supplementing hydrogels with carotenoids enhances their elastic properties

After treatment with chloroform, the color of the caudicles changed from orange to transparent, demonstrating the common role of carotenoids as pigments. However, the structural integrity and mechanical properties of caudicles also seemed to be compromised after chloroform treatment, suggesting that carotenoids might also be important structural components of caudicles and contribute to their elasticity. The causal relationship between carotenoids and elasticity of caudicles cannot be established at the moment because it is not possible to perform tensile test on the insoluble fraction after extraction. Nevertheless, inspired by the above results, we tried to use carotenoids to enhance the properties of existing elastomers. Freeze-drying and soaking experiments showed that caudicles are highly absorbent, containing 15% (w/w) water at harvest and 40% (w/w) water at saturation, which is similar to hydrogels. In addition, we have previously shown that the mechanical properties of caudicles are also very similar to that of hydrogels (Fig. 3e and f). Therefore, we synthesized calcium-alginate/polyacrylamide hydrogels that contain 0.50% (w/w) astaxanthin and compared their elastic properties with control hydrogels that do not contain astaxanthin (Fig. 5a). This hydrogel model is commonly used in previous studies [14,26–29]. We chose astaxanthin in our experiments because it is a typical oxygen-containing carotenoid. We tested astaxanthin concentrations of 0.00%, 0.03%, 0.05%, 0.10% and 0.50%, and chose 0.50% because tensile strength and breaking strain of hydrogels reach a plateau above 0.10% (Fig. S5). Raman spectroscopy confirmed that astaxanthin has been successfully incorporated into hydrogels (Fig. 5a). Tensile test showed that as compared with control hydrogels, the breaking strain and tensile strength of hydrogels containing astaxanthin are both significantly increased to two-fold (Fig. 5b–d). The elastic modulus and the slope of second linear segment are also slightly increased upon addition of astaxanthin (Fig. S6). This demonstrates that supplementing hydrogels with carotenoids can significantly enhance their elastic properties. We notice that the breaking strain of our control hydrogels (350%) is lower than that reported in literature (2200% and 1640%) [14,16], which is because of differences in synthesis protocol, especially the amount of covalent crosslinker MBAA, as well as differences in tensile test conditions, especially the size of hydrogel blocks (see Materials and Methods).

We proposed a model to explain the molecular basis of carotenoids' strengthening effect (Fig. 5e). Using astaxanthin as an example, each of the two terminal rings on the molecule is able to form two hydrogen bonds with alginate, polyacrylamide or another astaxanthin molecule (Fig. S7). In addition, the conjugated carbon-carbon double bonds in the carotenoid molecules can form larger conjugation systems with carboxyl and amino groups on polymer chains. Other weak intermolecular interactions such as coordinate bonds, p-π or π-π stacking and entanglement might also be involved in the system. Since the energy of hydrogen bonds (25–40 kJ/mol) is usually higher than that of other noncovalent interactions (less than 10 kJ/mol) [30], hydrogen bonds might be the major contributor to astaxanthin's strengthening effect, while other noncovalent interactions collectively might also contribute a significant amount. By forming multivalent weak interactions with polymer chains, carotenoids increase the degree of crosslinking between polymer chains, thereby increasing the tensile strength of hydrogels. Moreover, the crosslinks between carotenoids and polymer chains are reversible and can be redistributed during stretching, thereby increasing the breaking strain of hydrogels by effectively distributing stress across the gel and delaying the formation of stress concentration which is the major cause of fracture. This proposed mechanism is in line with a previous model that the strength of hydrogels can be increased by mixing weak and strong bonds [5,8,14–16,20,21,31].

4. Discussion

In this study, we identify the caudicle of vandoid orchids as an elastic plant tissue containing carotenoids. Although carotenoids commonly exist as monomers in living organisms, previous researches have shown that they can undergo oxidative polymerization and form polyperoxide or polyester [32]. The first naturally-occurring carotenoid polymer was discovered in the form of sporopollenin, the major component of pollen and spore exine [33–34]. Similar to sporopollenin, caudicles also originate from senescent tapetal cells during flower development [3,35], suggesting similar chemical structure and mechanism of formation. However, sporopollenin does not possess any degree of elasticity. Although our results suggest that caudicles contain carotenoid monomers, they do not exclude the possibility that carotenoid polymers exist in the insoluble fraction after chloroform treatment, *i.e.* the basal polymer fraction. Further study is needed to more thoroughly characterize the developmental process as well as the chemical structure of caudicles, including the identity and abundance of individual carotenoid species in the soluble fraction and the composition of the basal polymer fraction, in order to elucidate the role of carotenoids in the generation of elasticity in caudicles.

Our study also shows that carotenoids can be used as small molecule supplements in the synthesis of hydrogels to enhance their strength and stretchability, which might expand the biomedical and clinical applications of hydrogels. Hydrogels have been proposed to be used *in vivo* for tissue transplantation [36], wound healing [20] and drug delivery [37] purposes. Since different tissues have very different elastic moduli ranging from 0.1–0.2 kPa of neuronal cells to 10–100 kPa of bone or muscle cells [38], a way to fine-tune the mechanical properties of hydrogels is needed. As compared with other hydrogel enhancing strategies [14], carotenoids, being plant-derived, nontoxic and biocompatible, are excellent additives to hydrogels to alter their elastic properties for use in 3D cell culture and non-invasive injection. Previous studies suggest that such hydrogel additives, even when incorporated noncovalently, are able to retain within the hydrogel after *in vivo* administration [20].

In conclusion, our study suggests the presence of a carotenoid-based natural elastomer with low modulus, high extensibility and

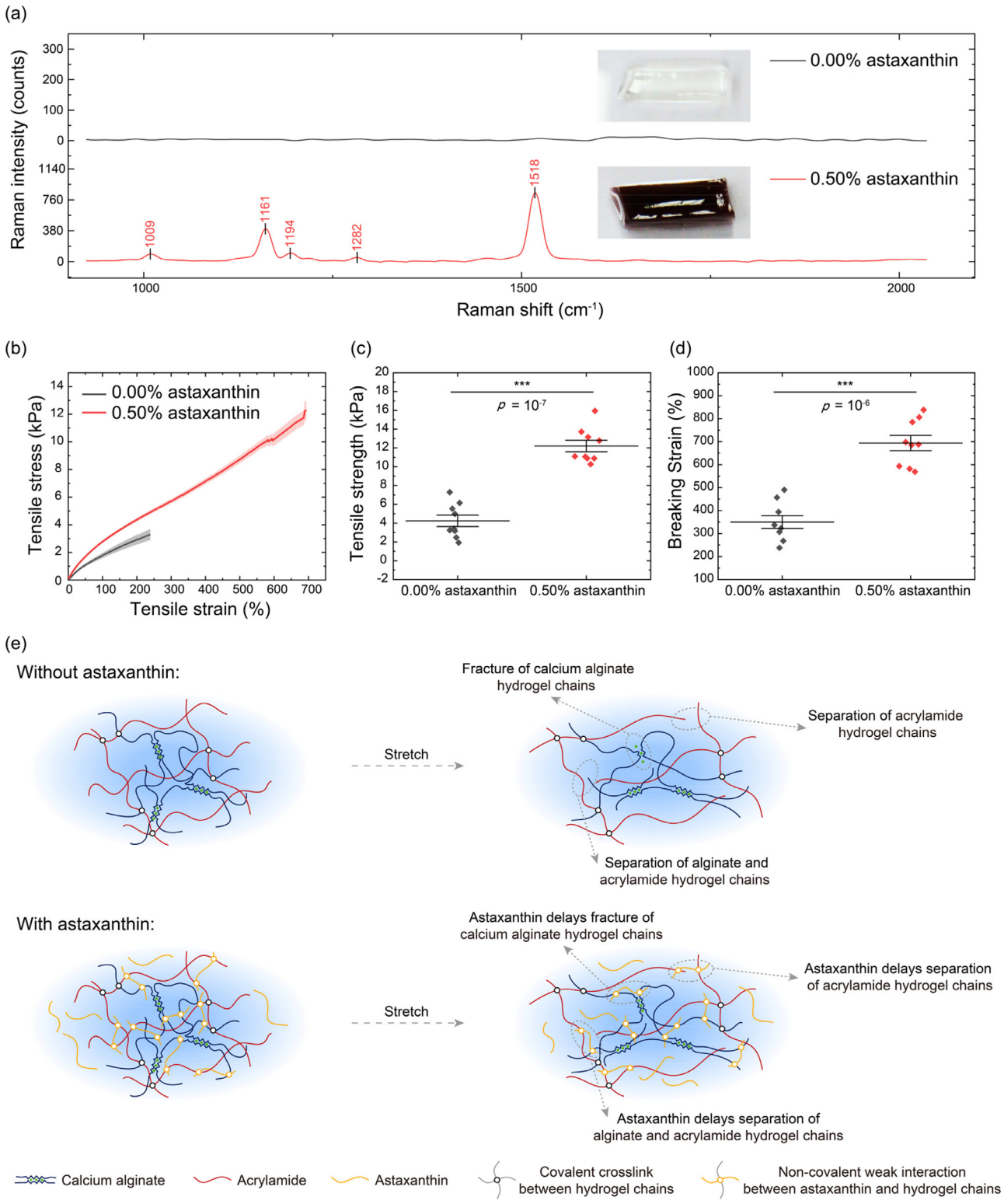

Fig. 5. Elastic properties of hydrogels supplemented with carotenoids. (a) Raman spectra of Ca-alginate-acrylamide hydrogels with 0.00% (black) and 0.50% (red) (w/w) astaxanthin. Insets, pictures of the two hydrogels. (b) Average stress-strain curve measured by tensile test (mean ± SEM; $N = 9$ for both samples). (c) Tensile strength of hydrogels. (d) Breaking strain of hydrogels. For (c) and (d), each dot represents one hydrogel block; $N = 9$ for both samples; means ± SEM are superimposed; two-tailed unpaired *t*-test is used for statistical analysis. (e) Schematic diagram of the molecular basis of carotenoids' strengthening effect. (For interpretation of the references to color in this figure legend, the reader is referred to the web version of this article.)

low density that are comparable with synthetic elastomers and approach the boundaries of the Ashby chart. Furthermore, we show that carotenoids can be used as reinforcing agents for synthetic hydrogels. Our findings provide basic knowledge and characterizations of caudicles as a natural material and demonstrate an important bio-inspired application of carotenoids in strengthening the mechanical properties of hydrogels.

5. Conclusion

In conclusion, this study investigates the microstructure, mechanical properties and chemical components of vandoid caudicles as an elastic plant tissue. Our results suggest that vandoid caudicles have homogenous inner structure on the micrometer scale, and that their morphology changes during flower development. Vandoid caudicles are more stretchable than most natural and synthetic elastomers and have modulus similar to hydrogels. The elasticity of vandoid caudicles is biologically relevant because it is manifested during pollination. Vandoid caudicles contain a mixture of carotenoid monomers that bind to basal polymers through noncovalent interactions. Furthermore, we show that supplementing astaxanthin, a typical carotenoid, to calcium-alginate/polyacrylamide hydrogels improves their strength and stretchability by two fold. Our findings provide basic knowledge and characterizations of caudicles as a natural material and demonstrate an important bio-inspired application of carotenoids in strengthening the mechanical properties of hydrogels.

Funding

This work was supported by the National Natural Science Foundation of China [grant numbers 11672037, 91848201, 11521202, 11988102]; Teaching Center for Experimental Biology of PKU; and the National Science Foundation for Fostering Talents in Basic Research of NSFC [grant number J1310033].

Declaration of Competing Interest

The authors declare that they have no known competing financial interests or personal relationships that could have appeared to influence the work reported in this paper.

Acknowledgments

The authors would like to thank Zhongxuan Wang, Kelin Liu, Ruidong Jia and Yan Wang for kindly providing plant materials.

Supplementary materials

Supplementary material associated with this article can be found, in the online version, at doi:10.1016/j.actbio.2020.07.005.

References

[1] R.L. Dressler, The Orchids: Natural History and Classification, Harvard University Press, Cambridge, MA, and London, 1981.
[2] C. Darwin, The Various Contrivances by Which Orchids are Fertilised by Insects, 2nd ed., J. Murray, London, 1890.
[3] E.C. Yeung, S.K. Law, The formation of hyaline caudicle in two vandoid orchids, Can. J. Bot. 65 (7) (1987) 1459–1464.
[4] R. Schill, M. Wolter, Ontogeny of elastoviscin in the Orchidaceae, Nord. J. Bot. 5 (6) (1986) 575–580.
[5] S. Abdurrahmanoglu, V. Can, O. Okay, Design of high-toughness polyacrylamide hydrogels by hydrophobic modification, Polymer 50 (23) (2009) 5449–5455.
[6] G. Jiang, C. Liu, X. Liu, Q. Chen, G. Zhang, M. Yang, F. Liu, Network structure and compositional effects on tensile mechanical properties of hydrophobic association hydrogels with high mechanical strength, Polymer 51 (6) (2010) 1507–1515.
[7] D.C. Tuncaboylu, M. Sari, W. Oppermann, O. Okay, Tough and self-healing hydrogels formed via hydrophobic interactions, Macromolecules 44 (12) (2011) 4997–5005.
[8] U. Gulyuz, O. Okay, Self-healing poly (acrylic acid) hydrogels with shape memory behavior of high mechanical strength, Macromolecules 47 (19) (2014) 6889–6899.
[9] M. Mihajlovic, M. Staropoli, M.S. Appavou, H.M. Wyss, W. Pyckhout-Hintzen, R.P. Sijbesma, Tough supramolecular hydrogel based on strong hydrophobic interactions in a multiblock segmented copolymer, Macromolecules 50 (8) (2017) 3333–3346.
[10] J. Yu, X. Chen, Y. Yang, X. Zhao, X. Chen, T. Jing, Y. Zhou, J. Xu, Y. Zhang, Y. Cheng, Construction of supramolecular hydrogels using imidazolidinyl urea as hydrogen bonding reinforced factor, J. Mater. Chem. B 8 (2020) 3058–3063.
[11] G.M. Pawar, M. Koenigs, Z. Fahimi, M. Cox, I.K. Voets, H.M. Wyss, R.P. Sijbesma, Injectable hydrogels from segmented PEG-bisurea copolymers, Biomacromolecules 13 (12) (2012) 3966–3976.
[12] J. Cui, A. del Campo, Multivalent H-bonds for self-healing hydrogels, ChemComm 48 (74) (2012) 9302–9304.
[13] M. Guo, L.M. Pitet, H.M. Wyss, M. Vos, P.Y. Dankers, E.W. Meijer, Tough stimuli-responsive supramolecular hydrogels with hydrogen-bonding network junctions, J. Am. Chem. Soc. 136 (19) (2014) 6969–6977.
[14] J.Y. Sun, X. Zhao, W.R.K. Illeperuma, O. Chaudhuri, K.H. Oh, D. Mooney, J.J. Vlassak, Z. Suo, Highly stretchable and tough hydrogels, Nature 489 (7414) (2012) 133–136.
[15] P. Lin, S. Ma, X. Wang, F. Zhou, Molecularly engineered dual-crosslinked hydrogel with ultrahigh mechanical strength, toughness, and good self-recovery, Adv. Mater. 27 (12) (2015) 2054–2059.
[16] C.H. Yang, M.X. Wang, H. Haider, J.H. Yang, J.Y. Sun, Y.M. Chen, J. Zhou, Z. Suo, Strengthening alginate-polyacrylamide hydrogels using various multivalent cations, ACS Appl. Mater. Interfaces 5 (2013) 10418–10422.
[17] K.J. Henderson, T.C. Zhou, K.J. Otim, K.R. Shull, Ionically cross-linked triblock copolymer hydrogels with high strength, Macromolecules 43 (2010) 6193–6201.
[18] X. Fang, J. Sun, One-step synthesis of healable weak-polyelectrolyte-based hydrogels with high mechanical strength, toughness, and excellent self-recovery, ACS Macro Lett. 8 (5) (2019) 500–505.
[19] T.L. Sun, T. Kurokawa, S. Kuroda, A.B. Ihsan, T. Akasaki, K. Sato, M.A. Haque, T. Nakajima, J.P. Gong, Physical hydrogels composed of polyampholytes demonstrate high toughness and viscoelasticity, Nat. Mater. 12 (10) (2013) 932–937.
[20] R. Bao, B. Tan, S. Liang, N. Zhang, W. Wang, W. Liu, A π-π conjugation-containing soft and conductive injectable polymer hydrogel highly efficiently rebuilds cardiac function after myocardial infarction, Biomaterials 122 (2017) 63–71.
[21] S.R. Shin, C. Zihlmann, M. Akbari, P. Assawes, L. Cheung, K. Zhang, V. Manoharan, Y.S. Zhang, M. Yüksekkaya, K.T. Wan, M. Nikkhah, Reduced graphene oxide-gelMA hybrid hydrogels as scaffolds for cardiac tissue engineering, Small 12 (27) (2016) 3677–3689.
[22] X. Zhao, Multi-scale multi-mechanism design of tough hydrogels: building dissipation into stretchy networks, Soft Matter 10 (5) (2014) 672–687.
[23] H. Yuk, B. Lu, X. Zhao, Hydrogel bioelectronics, Chem. Soc. Rev. 48 (6) (2019) 1642–1667.
[24] B. Lu, H. Yuk, S. Lin, N. Jian, K. Qu, J. Xu, X. Zhao, Pure PEDOT:PSS hydrogels, Nat. Commun. 10 (2019) 1043.
[25] J.C. Merlin, Resonance Raman spectroscopy of carotenoids and carotenoid-containing systems, Pure Appl. Chem. 57 (5) (1985) 785–792.
[26] H. Yuk, T. Zhang, S. Lin, G.A. Parada, X. Zhao, Tough bonding of hydrogels to diverse non-porous surfaces, Nat. Mater. 15 (2) (2016) 190–196.
[27] H.F. Chan, R. Zhao, G.A. Parada, H. Meng, K.W. Leong, L.G. Griffith, X. Zhao, Folding artificial mucosa with cell-laden hydrogels guided by mechanics models, Proc. Natl. Acad. Sci. USA 115 (29) (2018) 7503–7508.
[28] K. Zhang, C. Ma, Q. He, S. Lin, Y. Chen, Y. Zhang, N.X. Fang, X. Zhao, Metagel with broadband tunable acoustic properties over air–water–solid ranges, Adv. Funct. Mater. 29 (38) (2019) 1903699.
[29] J. Liu, S. Lin, X. Liu, Z. Qin, Y. Yang, J. Zang, X. Zhao, Fatigue-resistant adhesion of hydrogels, Nat. Commun. 11 (1) (2020) 1–9.
[30] J.H. Deng, J. Luo, Y.L. Mao, S. Lai, Y.N. Gong, D.C. Zhong, T.B. Lu, π-π stacking interactions: non-negligible forces for stabilizing porous supramolecular frameworks, Sci. Adv. 6 (2) (2020) eaax9976.
[31] Y. Huang, M. Zhong, Y. Huang, M. Zhu, Z. Pei, Z. Wang, Q. Xue, X. Xie, C. Zhi, A self-healable and highly stretchable supercapacitor based on a dual crosslinked polyelectrolyte, Nat. Commun. 6 (1) (2015) 1–8.
[32] G.W. Burton, J. Daroszewski, J.G. Nickerson, J.B. Johnston, T.J. Mogg, G.B. Nikiforov, β-Carotene autoxidation: oxygen copolymerization, non-vitamin A products, and immunological activity, Can. J. Chem. 92 (4) (2014) 305–316.
[33] J. Brooks, G. Shaw, Chemical structure of the exine of pollen walls and a new function for carotenoids in nature, Nature 219 (5153) (1968) 532–533.
[34] G. Shaw, The chemistry of sporopollenin, in: J. Brooks, P.R. Grant, M. Muir (Eds.), Sporopollenin, Academic Press, Cambridge, MA, 1971, pp. 305–350.
[35] P. Echlin, Production of sporopollenin by the tapetum, in: J. Brooks, P.R. Grant, M. Muir (Eds.), Sporopollenin, Academic Press, Cambridge, MA, 1971, pp. 220–247.
[36] K.Y. Lee, D.J. Mooney, Hydrogels for tissue engineering, Chem. Rev. 101 (7) (2001) 1869–1880.
[37] F. Li, Y. Zhu, B. You, D. Zhao, Q. Ruan, Y. Zeng, C. Ding, Smart hydrogels co-switched by hydrogen bonds and π–π stacking for continuously regulated controlled-release system, Adv. Funct. Mater 20 (4) (2010) 669–676.
[38] E.M. Darling, D. Di Carlo, High-throughput assessment of cellular mechanical properties, Annu. Rev. Biomed. Eng. 17 (2015) 35–62.